CHAPTER IV
RESULTS AND DISCUSSION

4.1 Catalyst Characterization

4.1.1 BET Surface Area and Nickel Dispersion

The BET surface areas of the catalysts are listed in Table 4.1. The BET surface areas of the catalysts are in the range of 39 – 93 m^2/g. The surface area of CZO is 93.68 m^2/g. When Ni was impregnated, the surface area was decreased to 73.74 m^2/g. Ni impregnation on the supports causes a decrease in the surface area, this behavior could be attributed to the blockade of the pores in the support by the Ni (Perez *et al.*, 2011). For all catalysts, the surface areas were decreased with increasing Mn wt% content. It might be due to the pore blockage by Mn. Additionally, the multi-step incipient wetness impregnation catalysts show slightly decrease on surface area compare with co-impregnation catalysts. This might be suggested that the nickel dispersion for the multi-step incipient wetness impregnation catalysts were highly dispersed than that of the co-impregnation catalysts. It was confirmed with the degrees of nickel dispersion of catalysts as shown in Table 4.1.

The degree of Nickel dispersions of catalysts were in the range of ca. 4 – 6%. The degree of dispersion of Ni/CZO was about 6%. The Ni metal dispersions were slightly decreased with increasing amount of Mn on both preparation methods. No adsorption of H_2 on Mn/CZO was detected. It should be noticed that manganese partially covered on nickel surface (Pengpanich *et al.*, 2008).

Table 4.1 BET surface areas and degrees of nickel dispersion of the catalysts

Catalyst	Surface Area (m^2/g)	Ni metal dispersion (%)
CZO	93.68	-
Ni/CZO	73.74	6.15
15Ni5Mn/CZO (C)	43.07	6.04
15Ni10Mn/CZO (C)	41.04	4.09
15Ni15Mn/CZO (C)	39.23	3.56
15Ni5Mn/CZO (S)	51.25	6.05
15Ni10Mn/CZO (S)	45.22	5.43
15Ni15Mn/CZO (S)	41.01	4.92

4.1.2 X-ray Diffraction (XRD)

The XRD patterns of catalysts after calcinations at 500°C are shown in Figure 1. The catalysts exhibited the major peaks indicated two phases such a cubic fluorite structure of CeO_2 exhibited at about 28°, 33°, 48° and 57° and NiO phase exhibited at about 37°, 43°, and 62° (Bempenrat *et al.*, 2010). The results showed no distinguished peaks of both MnO_2 which were reported in the case of Jose *et al.*, 2007. This is due to an overlapping of XRD patterns of CeO_2 and NiO. The XRD patterns also confirmed that there is no Ni-Mn solid solution occurred as Ryazhkin *et al.*, 2009.

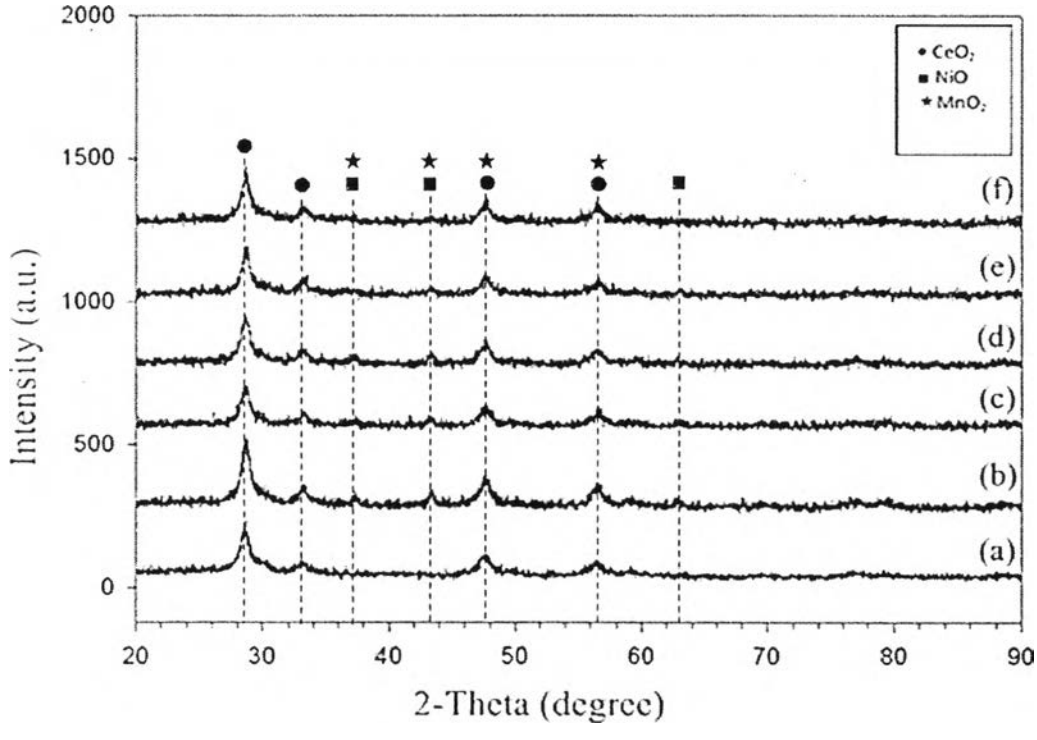

Figure 4.1 XRD patterns for the catalysts: (a) CZO (b) 15Ni/CZO (c) 15Ni5Mn/CZO (C) (d) 15Ni15Mn/CZO (C) (e) 15Ni5Mn/CZO (S) (f) 15Ni15Mn/CZO (S).

4.1.3 Scanning Electron Microscopy (SEM)

Figure 4.2 shows the SEM images of fresh 15Ni/CZO, 15Ni5Mn/CZO (C), and 15Ni5Mn/CZO (S) catalysts. The Ni particle size of the samples is in the range of 20 - 40 nm.

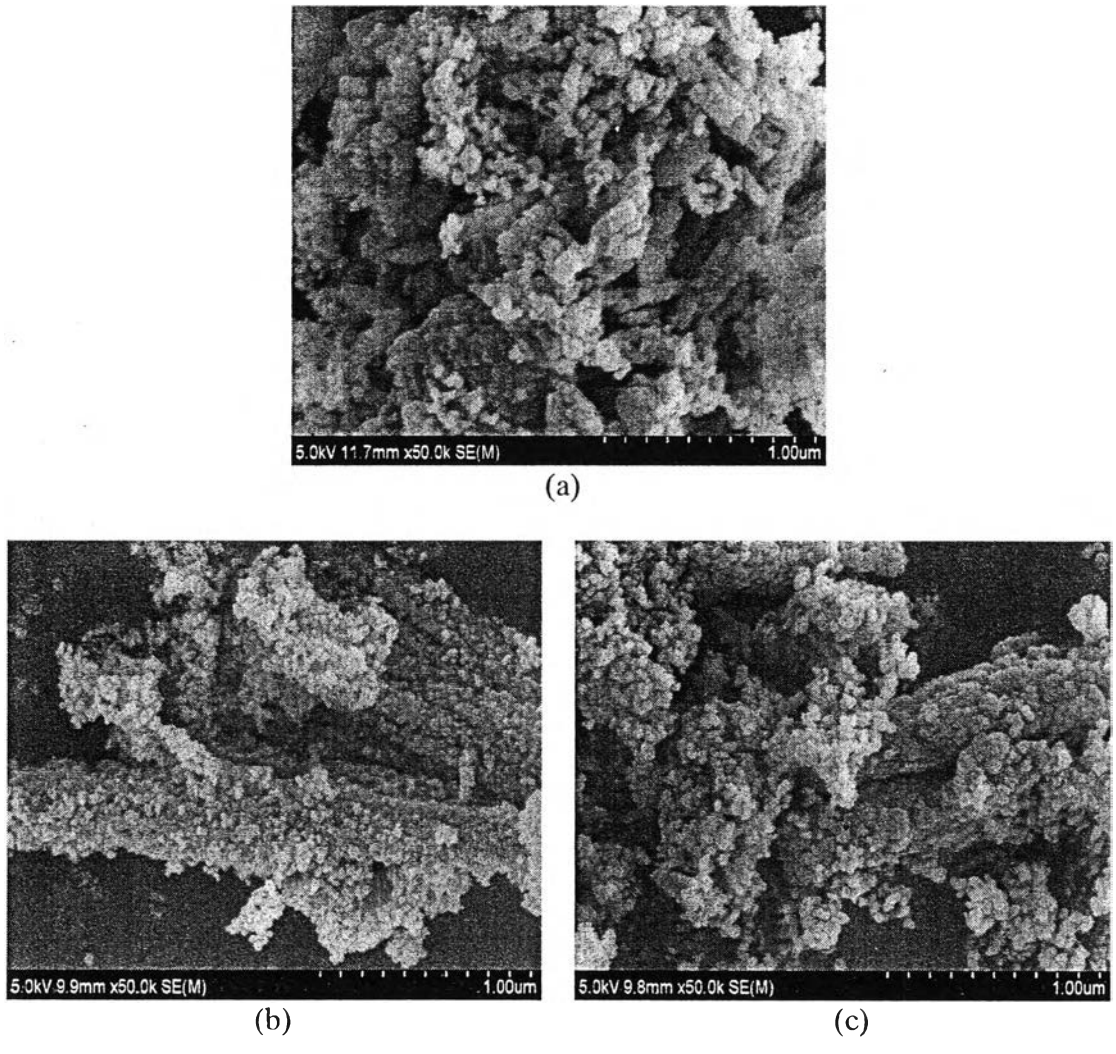

Figure 4.2 SEM images of fresh catalysts; (a) 15Ni/CZO (b) 15Ni5Mn/CZO (C) (c) 15Ni5Mn/CZO (S).

4.1.4 Temperature-Programmed Reduction by Hydrogen (H_2-TPR)

H_2-TPR profiles of catalysts are shown in Figure 4.2. The TPR profile of the CZO support shows the reduction peak of CeO_2 at about 550°C. The Ni/CZO catalyst shows two reduction peaks that clearly observed at 260 and 380°C. The first can be associated with the reduction of free NiO particles and other peak can be ascribed to the reduction of complex NiO species in intimate contact with the oxide support (Penpanich *et al.*, 2004). The reduction peaks of Mn/CZO exhibit two temperatures at 320°C attributed to the reduction of MnO_2 to Mn_2O_3, and other peak appearing at 400°C was ascribed to the reduction of MnO_2/Mn_2O_3 to Mn_3O_4 (Wu *et al.*, 2004, Kip *et al.*, 1987 and Park *et al.*, 2010).

The TPR profiles of Ni-Mn/CZO catalysts prepared via co-impregnation method are shown in Figure 4.3 and prepared via multi-step impregnation are shown in Figure 4.4. There are one main peak at high temperature and some shoulder peaks at lower temperature. At higher peak (380 – 400°C) represents the reduction of complex NiO interacted with CZO. This peak shifts to higher temperature with an increase in Mn loading indicating the weaker interaction of NiO and support. It might be lead to lowering dispersion of nickel, as evidenced by the following H_2 chemisorptions results (Dong *et al.*, 2002). Besides disperse MnO_x species bulk α-Mn_2O_3 are also present in the mixed oxides. These species reduce at about 300°C to Mn_3O_4. This shoulder peak is more clearly observed at high amount of Mn loading. The 15Ni5Mn/CZO (S) was show the best reduction of Ni as well as Mn-promoted catalysts. In this result, there are no significantly distinguish of TPR profiles on both preparation methods. Moreover, the MnO_x species did not interfere with the support interactions between NiO and the ceria– zirconia based on TPR results.

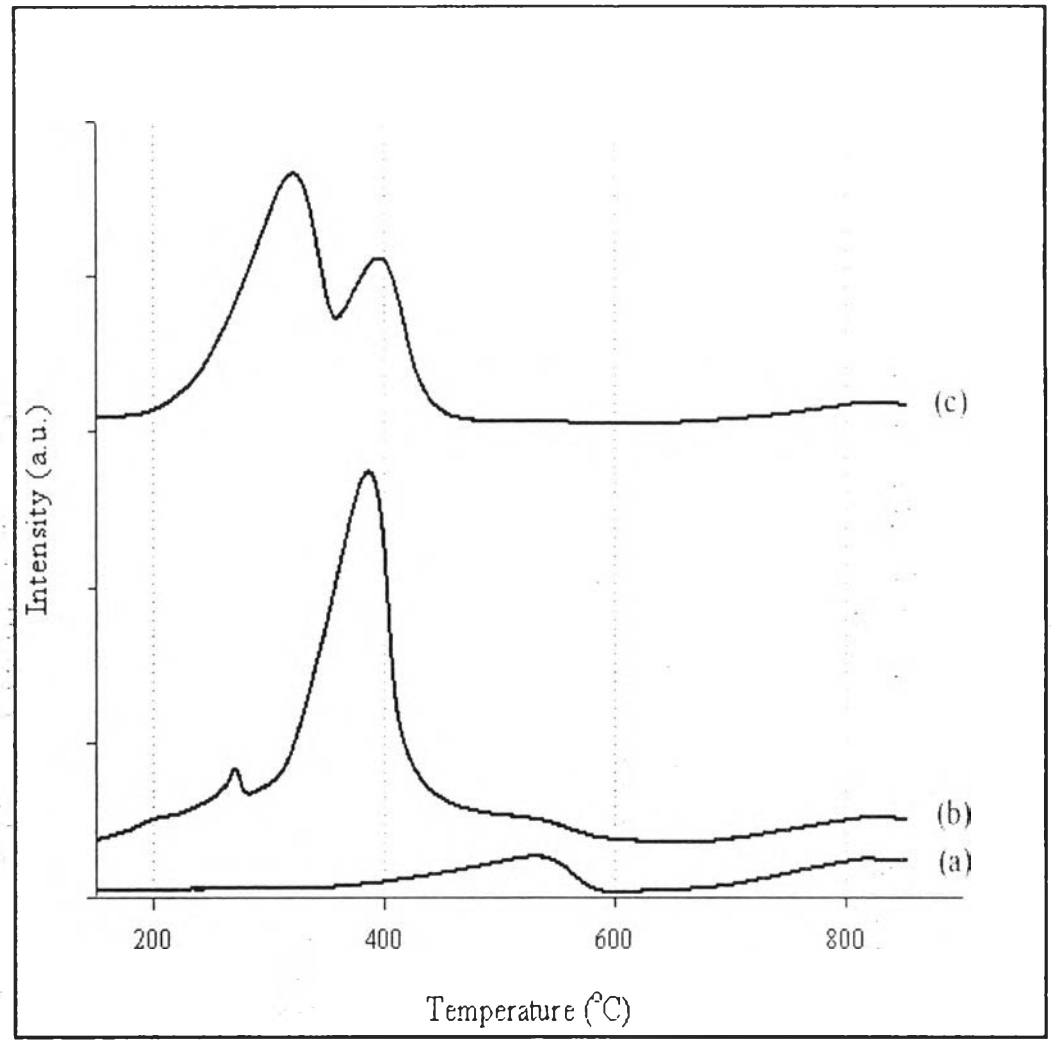

Figure 4.3 H_2-TPR profiles of catalysts with heating rate of 10°C min^{-1}, a reducing gas containing 5% H_2 in N_2 with a flow rate of 20 ml min^{-1}; (a) CZO (b) 15Ni/CZO (c) 15Mn/CZO.

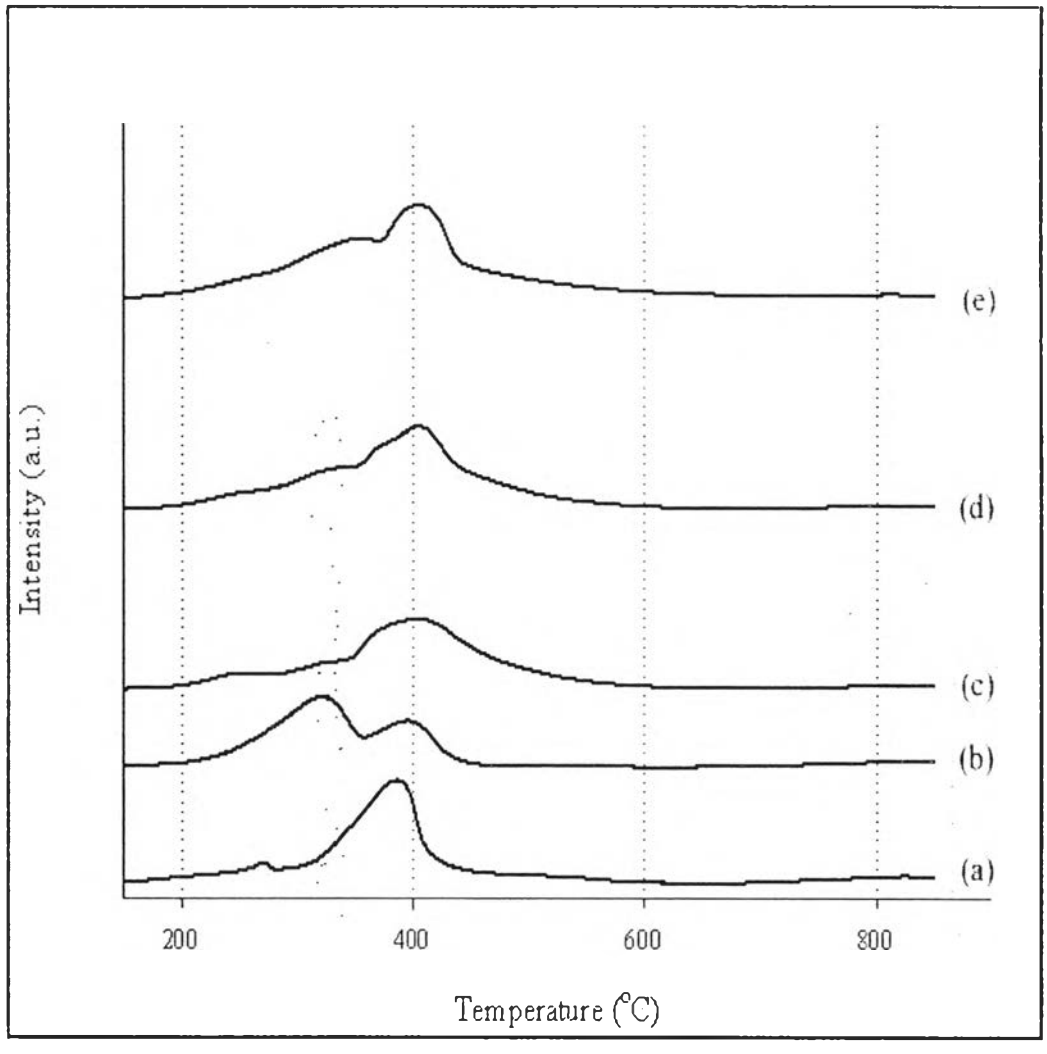

Figure 4.4 H_2-TPR profiles of catalysts with heating rate of 10°C min^{-1}, a reducing gas containing 5% H_2 in N_2 with a flow rate of 20 ml min^{-1}; (a) 15Ni/CZO (b) 15Mn/CZO (c) 15Ni5Mn/CZO (C) (d) 15Ni10Mn/CZO (C) (e) 15Ni15Mn/CZO (C).

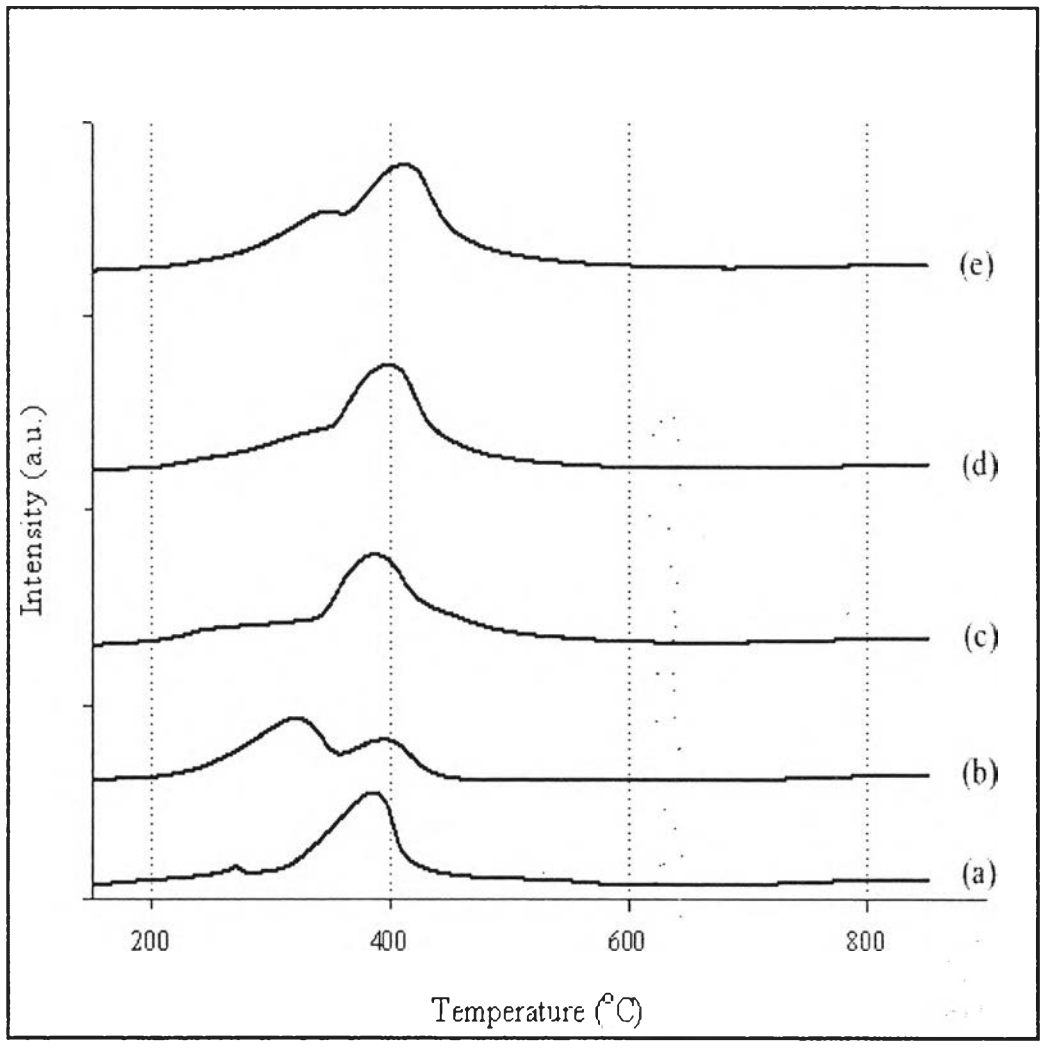

Figure 4.5 H_2-TPR profiles of catalysts with heating rate of 10°C min^{-1}, a reducing gas containing 5% H_2 in N_2 with a flow rate of 20 ml min^{-1}; (a) 15Ni/CZO (b) 15Mn/CZO (c) 15Ni5Mn/CZO (S) (d) 15Ni10Mn/CZO (S) (e) 15Ni15Mn/CZO (S).

4.2 Catalytic Activity on Methane Steam Reforming

4.2.1 Effect of Temperature

Figure 4.6 presents the methane conversion on MSR as a function of time over Ni-Mn/CZO catalysts at 700°C and S/C = 4/1. The CH_4 conversion over Ni/CZO started at 75% and decreased to 65% after 5 h. For Ni-Mn/CZO prepared via co-impregnation method, the initial methane conversions were dramatically decreased from 78% to 55% over 5% and 15% Mn loading. It might be due to the decreasing in Ni active sites which partially coverage by Mn as indicated by metal dispersion. The Ni-Mn/CZO prepared via multi-step impregnation catalysts showed a superior activity over the other catalyst especially 5% Mn loading as a result of higher Ni metal dispersion. It should be note that Ni surface areas are increased. However the 10 and 15% Mn loading prepared via this method showed slightly decrease in conversion. This is accordance with the reduction temperature of Ni, which indicates that harder the reduction catalysts. When the reaction temperature increased to 800°C, the CH_4 conversion over Ni/CZO was increased to 82% as show in Figure 4.9. For all Mn-promoted catalysts, the methane conversions on MSR at 800°C were lower than that from 78% to 55% over 5% and 15% Mn loading. There is a marginal decrease in the activity of Mn-promoted catalysts in spite of the partial blockage of the nickel surface. However, the 5% Mn loading prepared via multi-step impregnation method provide slightly higher conversion than that of the co-impregnation catalysts at higher temperature.

Figure 4.7 and 4.9 show the hydrogen yield on MSR over Ni-Mn/CZO catalysts at 700 and 800°C, respectively. The H_2 yield of Ni/CZO is approximately 80% increased upto 86 and 87% over 15Ni5Mn/CZO (C) and 15Ni5Mn/CZO (S), respectively. That might be due to the Mn promoted the water gas shift reaction occurred (Bampenrat *et al.*, 2010) confirmed with high H_2/CO ratio and lower CO selectivity as Figure 4.7. Additionally, hydrogen yield of the 10 and 15% Mn loading via multi-step impregnation were higher than co-impregnation. That might be due to

higher conversion over multi-step impregnation catalysts. At 800°C, the Ni/CZO catalysts gave higher hydrogen yield (~88%) due to higher conversion. The hydrogen yield over all Mn-promoted catalysts provide slightly decreased with increasing in Mn loading. It might be due to the lower of methane conversion. However, the Mn-promoted catalysts were still provided high hydrogen yield due to the water gas shift reaction still occurred (Bampenrat *et al.*, 2010) at higher temperature. That might be confirmed with either lower CO selectivity or high H_2/CO ratio. Additionally, the selectivity of CO over 10 wt% Mn loading catalysts on both methods is much lower than that over 15Ni/CZO, while the H_2/CO ratio is much higher that similar to activity at 700°C.

The CO selectivity and H_2 to CO ratio on MSR over Ni-Mn/CZO catalysts are shown in Figure 4.8 and Figure 4.9. The selectivity of CO over 10% Mn-Ni/CZO catalyst on multi-step impregnation method is much lower than that over 15Ni/CZO, while the H_2/CO ratio is much higher. The H_2/CO ratio over the catalyst is approximately 8.8, indicating that the water–gas shift (WGS) reaction occurs.

The lower of activity on MSR over Ni-Mn/CZO catalysts might be caused by the formation of MnO on an alumina support reported by Jacono *et al.*, 1976. However, this phase may be that of manganese interacting with $CeZrO_2$ support and the manganese oxide species actually decorating nickel particles may be in a different oxidation state (Seok *et al.*, 2001). Another reason might be due to the sintering of the metals on surface of catalysts.

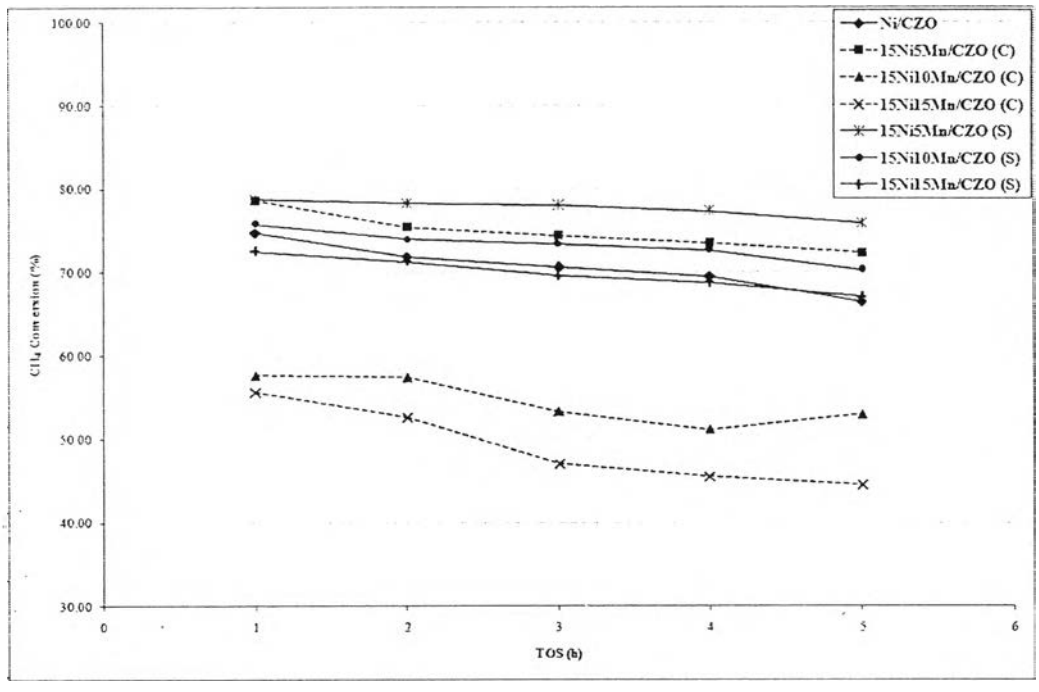

Figure 4.6 CH_4 conversion on MSR over Ni-Mn/CZO catalysts at 700°C and S/C ratio = 4/1 (GSHV = 42000 h^{-1}).

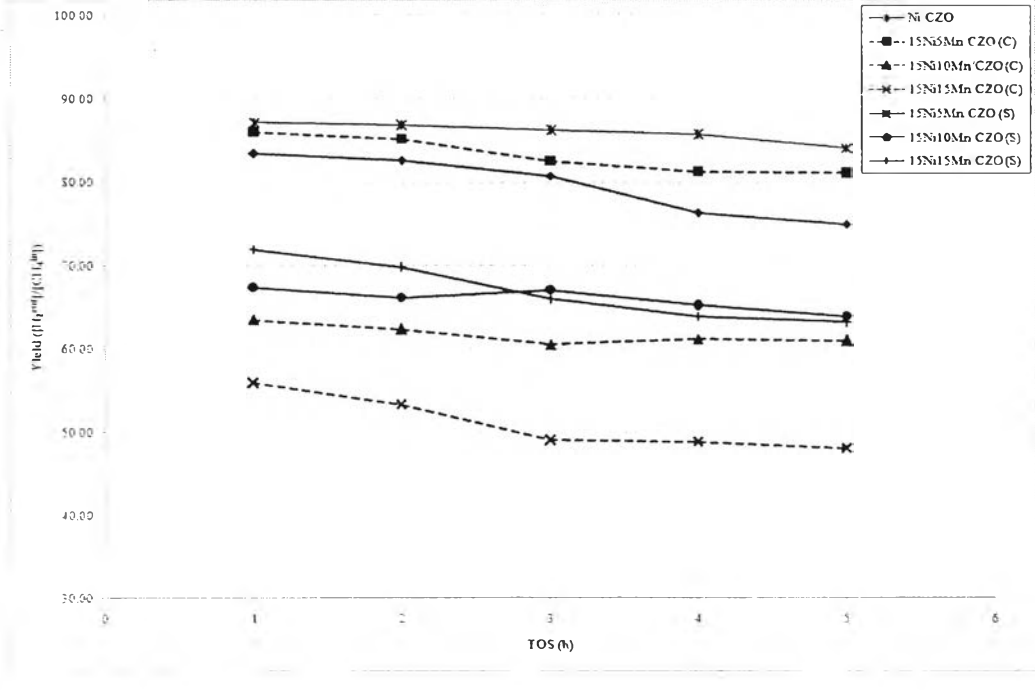

Figure 4.7 H_2 yield on MSR over Ni-Mn/CZO catalysts at 700°C and S/C ratio = 4/1 (GSHV = 42000 h^{-1}).

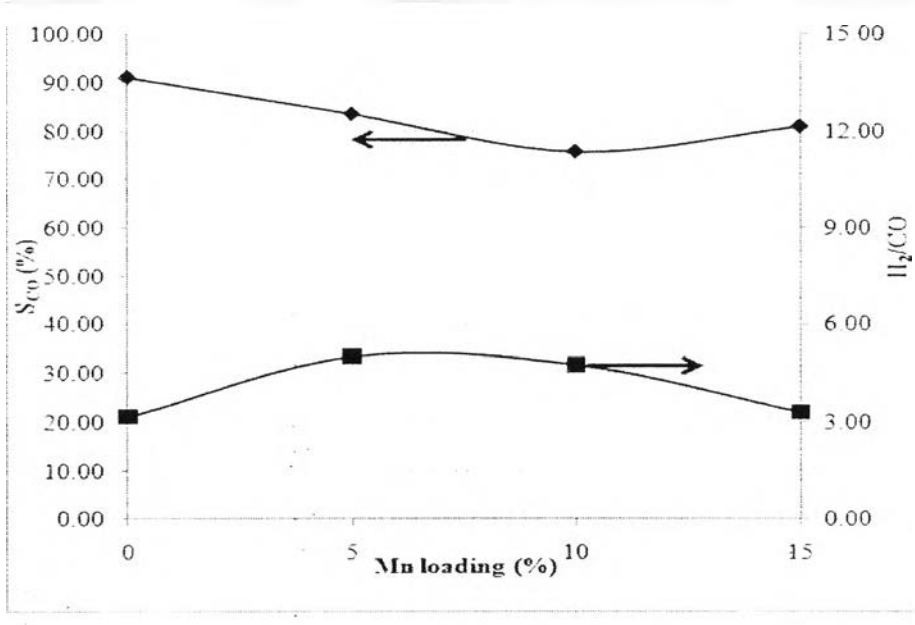

(a)

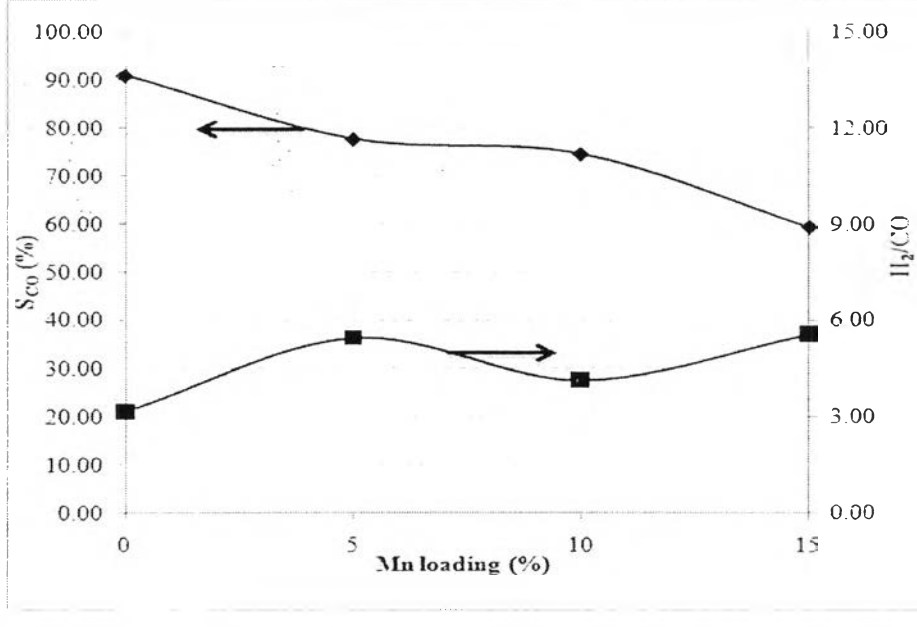

(b)

Figure 4.8 CO selectivity and H_2/CO on MSR over Ni-Mn/CZO catalysts at 700°C, S/C ratio = 4/1, and TOS = 3 h (GSHV = 42000 h^{-1}); (a) Co-impregnation method (b) Multi-step impregnation method.

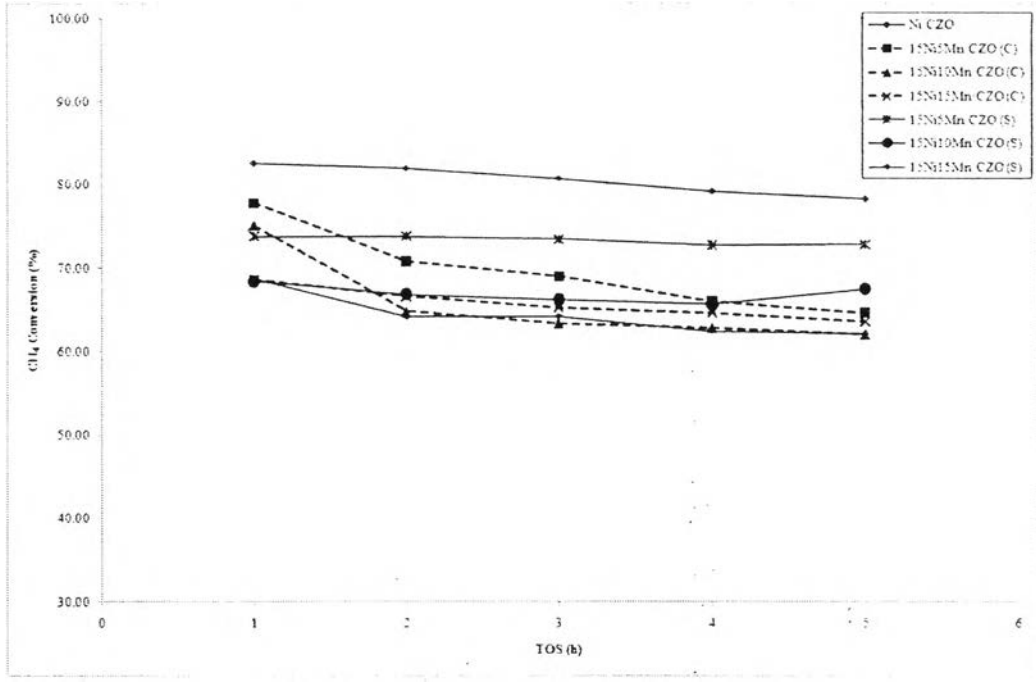

Figure 4.9 CH_4 conversion on MSR over Ni-Mn/CZO catalysts at 700°C and S/C ratio = 4/1 (GSHV = 42000 h^{-1}).

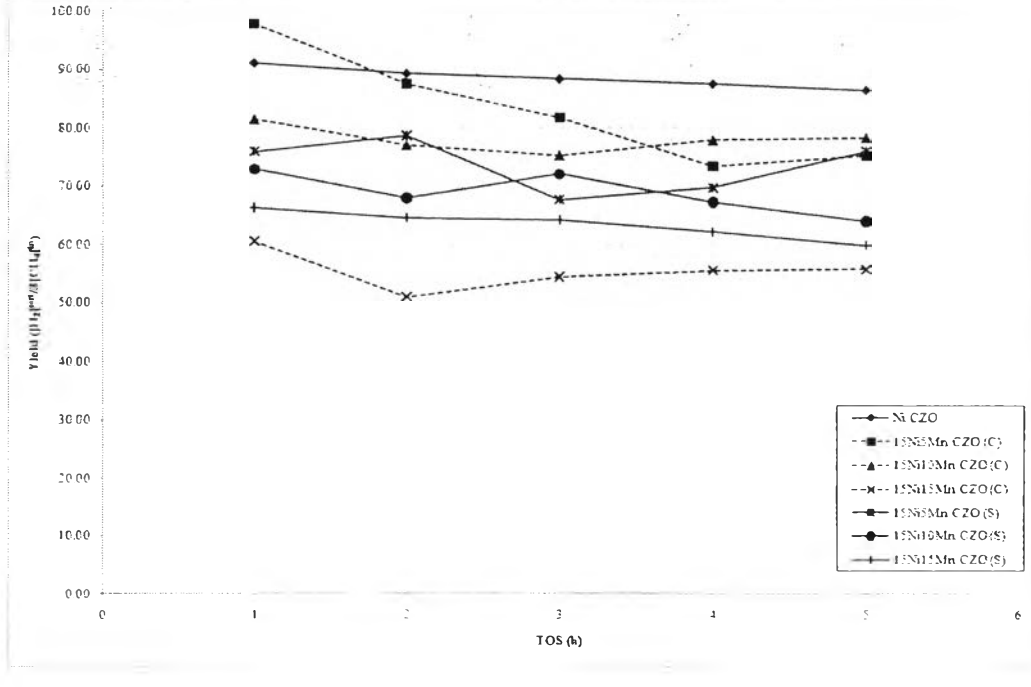

Figure 4.10 H_2 yield on MSR over Ni-Mn/CZO catalysts at 800°C and S/C ratio = 4/1 (GSHV = 42000 h^{-1}).

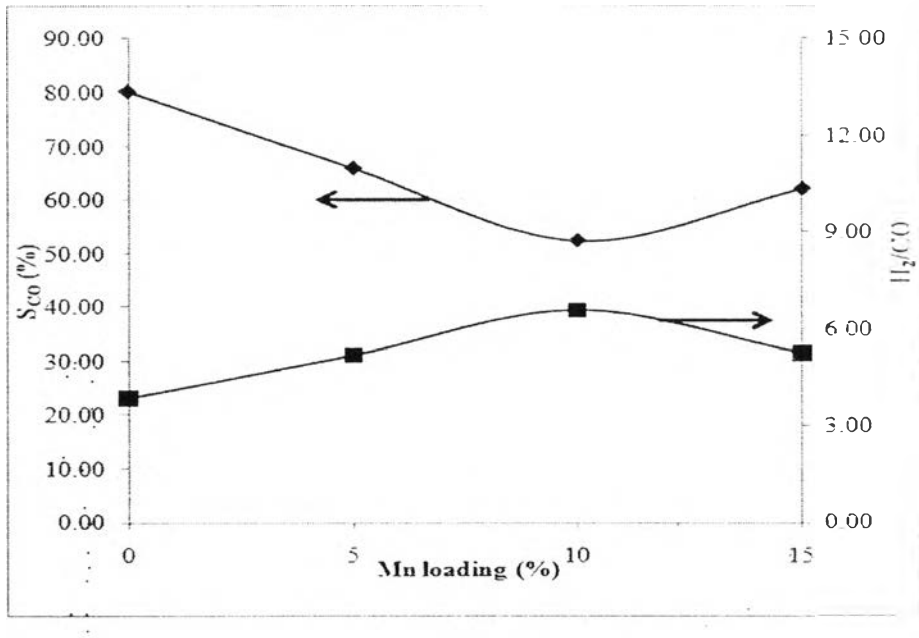

(a)

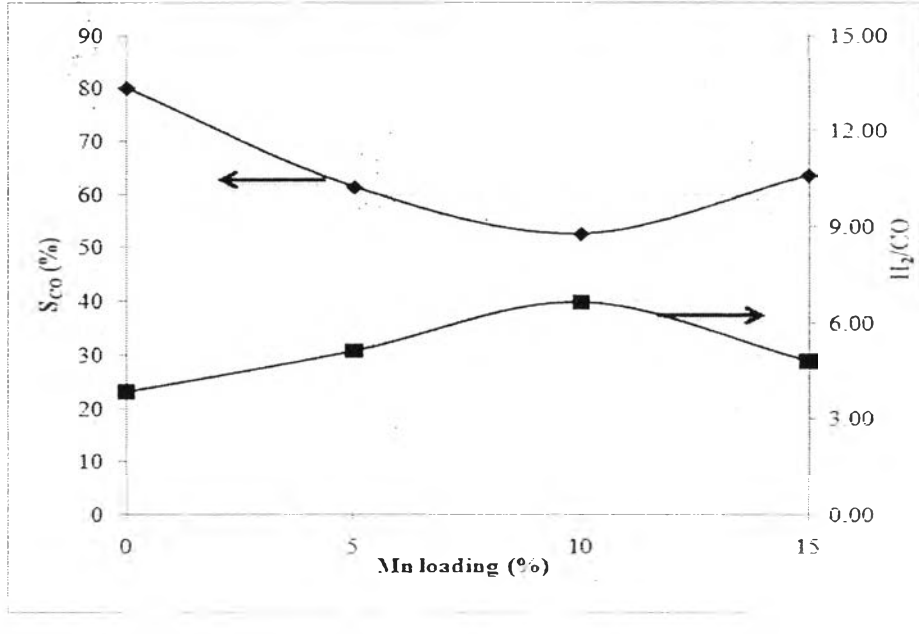

(b)

Figure 4.11 CO selectivity and H_2 yield on MSR over Ni-Mn/CZO catalysts at 800°C, S/C ratio = 4/1, and TOS = 3 h (GSHV = 42000 h^{-1}); (a) Co-impregnation method (b) Multi-step impregnation method.

4.2.2 Effect of Steam to Carbon Ratio

The effect of steam to carbon ratio was investigated on S/C = 4/1 and 3/1 over Ni/CZO and 5% Mn loading of both preparation methods at reaction temperature = 600°C. The results show that the 15Ni5Mn/CZO (S) gave the highest methane conversion on MSR at both S/C = 4/1 and 3/1 as show in Figure 4.12 and 4.13, respectively. At S/C equal 4, the methane conversion was drop after 5 hours contrast with Mn-promoted catalysts. At low steam to carbon ratio, the methane conversion over Ni/CZO catalyst dramatically decreased. It might be due to rapidly of carbon growth and completely inhibit the reaction after 1 hour. The methane conversion over 15Ni5Mn/CZO (C) was also decreased about 10% and completely inhibited reaction after 1.30 hour. It is apparent that 15Ni5Mn/CZO (S) could diminish the carbon deposition resulting in the activity at low temperature and steam to carbon ratio of the catalyst.

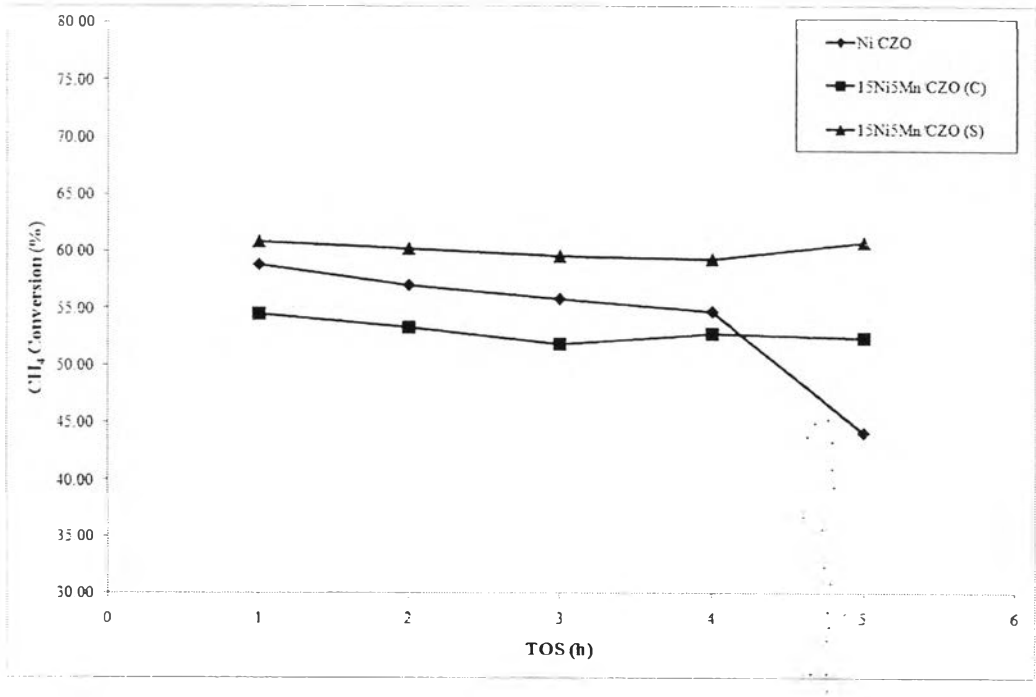

Figure 4.12 CH_4 conversion on MSR over Ni-Mn/CZO catalysts at 600°C and S/C ratio = 4/1 (GSHV = 42000 h^{-1}).

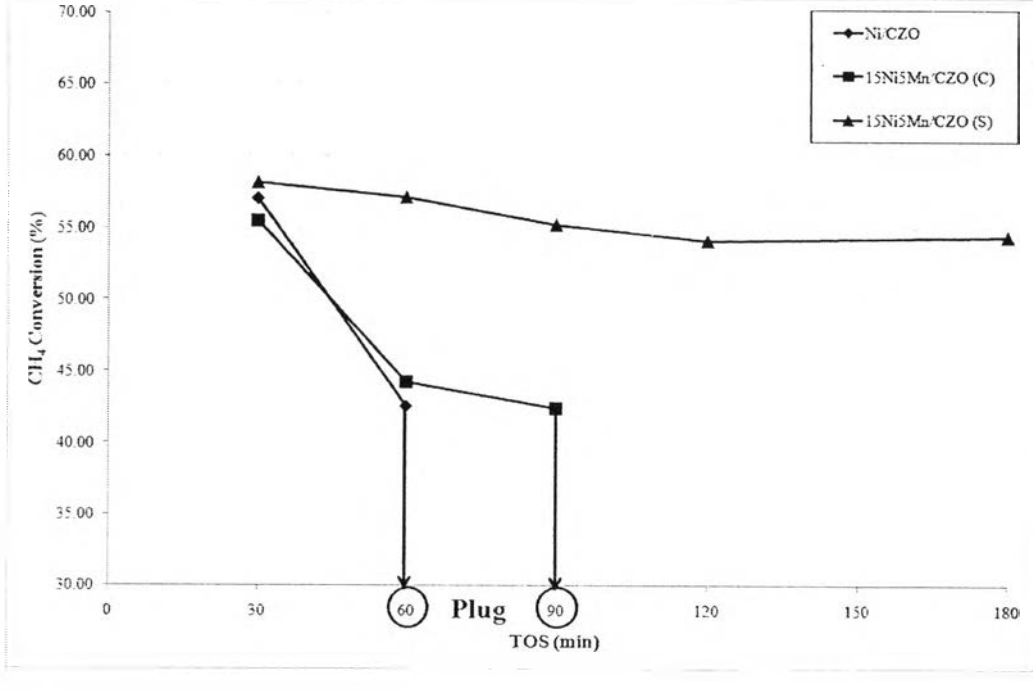

Figure 4.13 CH_4 conversion on MSR over Ni-Mn/CZO catalysts at 600°C and S/C ratio = 3/1(GSHV = 42000 h^{-1}).

4.3 Carbon Deposition on Spent Catalysts

The amounts of carbon depositions on catalysts, quantified by TPO technique, are shown in Table 4.2 and 4.3. As shown in table 4.2, the amount of carbon deposition was decreased rapidly by Mn-promoted via sequential impregnation method. In contrast with the co-impregnation catalysts, it was showed the slightly decreased in carbon deposition on spent catalysts. It might be noticed that 10 and 15 Mn loading provided the low reaction activity that lead to the less carbon deposition on spent catalysts. However, the carbon deposition on SMR at 700°C after 6 h show very less the lower reaction temperature and lower S/C ratio should further investigated. The results show that after 3 h on SMR at 600°C and S/C = 3/1 the tendency of carbon deposition was similarly to previous reaction condition. The 15Ni8Mn/CZO (S) show the best reduction on coke formation.

From prior results of characterization it might be postulated that a large part of the surface Ni atoms was blocked by MnO_x, as was proposed for impregnated 5%Ni/10%MnO/Al_2O_3 (Seok, 2001). Such a partial blockage of nickel surface would suppress the coke deposition because the ensemble size necessary for carbon formation is larger than that required for methane reforming (Bradford, 1999). The images of SEM of spent catalysts after 6 h on SMR at 700°C and S/C = 4/1 are show in Figure 4.14. It was observed that the filamentous carbon was formed on Ni/CZO catalysts, while no carbon was formed on both preparation methods of Ni-Mn/CZO catalysts. Additionally, the SEM images of spent catalysts after severity condition are shown in Figure 4.15, the 15Ni5Mn/CZO (S) was confirmed to retarding carbon formation on spent catalysts.

Table 4.2 Amount of coke formation over catalysts after 6 h on MSR at 700°C and S/C ratio of 4/1 (GSHV = 42000 h^{-1})

Catalysts	Coke Formation (%)
Ni/CZO	0.17
15Ni5Mn/CZO (C)	0.18
15Ni10Mn/CZO (C)	0.12
15Ni15Mn/CZO (C)	0.05
15Ni5Mn/CZO (S)	0.03
15Ni10Mn/CZO (S)	0.06
15Ni15Mn/CZO (S)	0.08

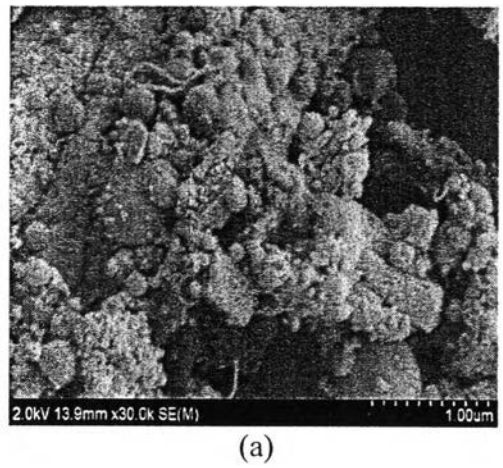

(a)

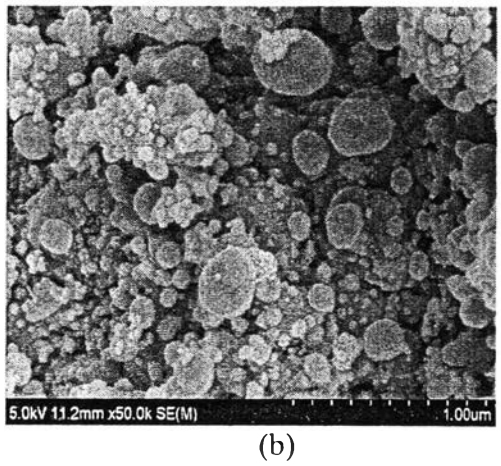

(b)

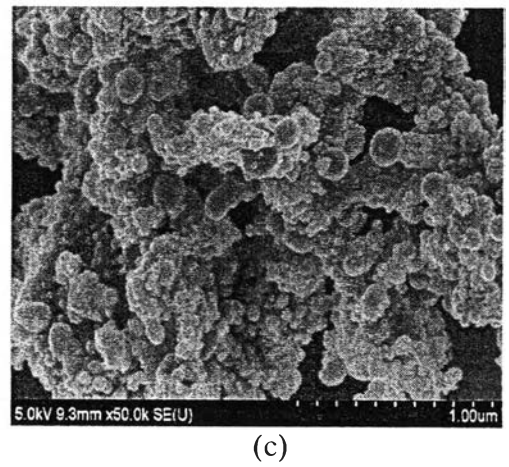

(c)

Figure 4.14 SEM images of spent catalysts after MSR reaction at 700°C and S/C ratio of 4/1; (a) Ni/CZO (b) 15Ni5Mn/CZO (C) (c) 15Ni5Mn/CZO (S).

Table 4.3 Amount of coke formation over catalysts after 3 h on MSR at 600°C and S/C ratio of 3/1 (GSHV = 42000 h^{-1})

Catalysts	Coke Formation (%)
Ni/CZO	42.5
15Ni5Mn/CZO (C)	39.6
15Ni5Mn/CZO (S)	24.0

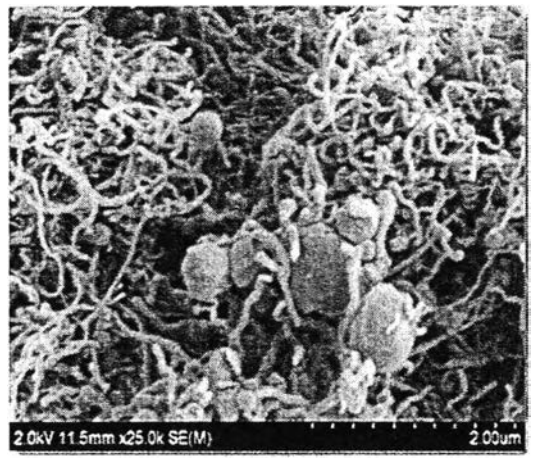

(a)

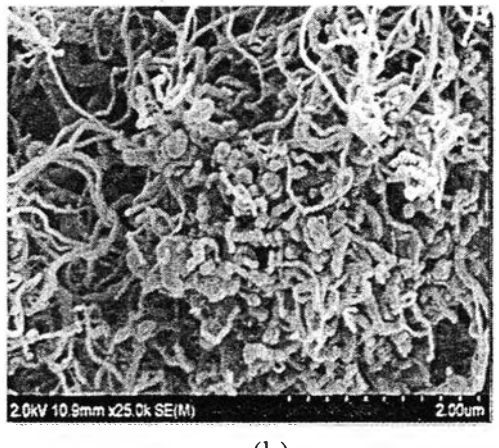

(b)

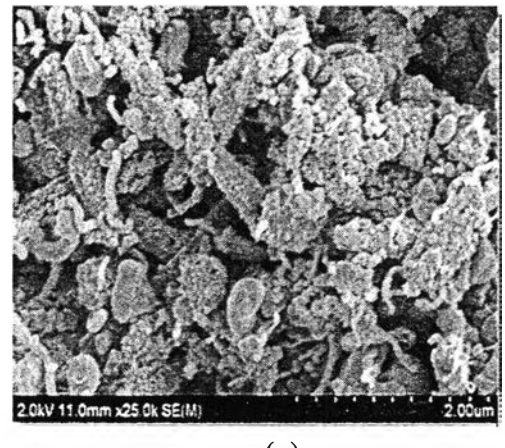

(c)

Figure 4.15 SEM images of spent catalysts after MSR reaction at 600°C and S/C ratio of 3/1; (a) Ni/CZO (b) 15Ni5Mn/CZO (C) (c) 15Ni5Mn/CZO (S).